

Molecular Interactions in 1-Ethyl-3-Methylimidazolium Tetrafluoroborate + Amide Mixtures: Excess Molar Volumes, Excess Isentropic Compressibilities and Excess Molar Enthalpies

V. K. Sharma · Soniya Bhagour

Received: 8 June 2012 / Accepted: 20 September 2012 / Published online: 10 April 2013
© Springer Science+Business Media New York 2013

Abstract The densities, ρ_{12} , and speeds of sound, u_{12} , of 1-ethyl-3-methylimidazolium tetrafluoroborate (1) + *N*-methylformamide or *N,N*-dimethylformamide (2) binary mixtures at (293.15, 298.15, 303.15, 308.15 K), and excess molar enthalpies, H_{12}^E , of the same mixtures at 298.15 K have been measured over the entire mole fraction range using a density and sound analyzer (Anton Paar DSA-5000) and a 2-drop microcalorimeter, respectively. Excess molar volume, V_{12}^E , and excess isentropic compressibility, $(\kappa_S^E)_{12}$, values have been calculated by utilizing the measured density and speed of sound data. The observed data have been analyzed in terms of: (i) Graph theory and (ii) the Prigogine–Flory–Patterson theory. Analysis of the V_{12}^E data in terms of Graph theory suggest that: (i) in pure 1-ethyl-3-methylimidazolium tetrafluoroborate, the tetrafluoroborate anion is positioned over the imidazolium ring and there are interactions between the hydrogen atom of (C–H{edge}) and proton of the $-\text{CH}_3$ group (imidazolium ring) with fluorine atoms of tetrafluoroborate anion, and (ii) (1 + 2) mixtures are characterized by ion–dipole interactions to form a 1:1 molecular complex. Further, the V_{12}^E , H_{12}^E and $(\kappa_S^E)_{12}$ values determined from Graph theory compare well with their measured experimental data.

Keywords Excess molar volumes V^E · Excess molar enthalpies H^E · Excess isentropic compressibilities κ_S^E · Connectivity parameter of third degree of a molecule ${}^3\xi$ · Interaction parameter χ

1 Introduction

The increasing interest in ionic liquids has led to research activities concerning thermodynamics and thermophysical properties of ionic liquid mixtures. Ionic liquids are comprised of a large organic cation and an inorganic polyatomic anion. In recent years they have also been considered as designer solvents as their physical properties can be tuned by

V. K. Sharma (✉) · S. Bhagour
Department of Chemistry, M. D. University, Rohtak 124001, India
e-mail: v_sharmachem58@rediffmail.com

careful selection of the anion or cation. They are widely used in many industrial processes such as organic synthesis, electrochemistry, separation processes, multiphase separation, etc. [1–4]. The physical and thermodynamic properties of an ionic liquid depend mostly on the nature and size of both their cation and anion constituents [5–7]. The chemical complexity of the cation and anion involved in the liquid structure also exhibit a challenge for theoreticians to understand thermodynamic properties of ionic liquids mixtures on the basis of molecular interactions. However, in spite of their practical importance, there is a considerable lack of data on thermodynamic properties [8–10] like V^E , H^E and κ_S^E of ionic liquid mixtures.

We are unaware of any V_{12}^E , H_{12}^E and $(\kappa_S^E)_{12}$ data of our studied mixtures with which the experimental data can be compared.

The topology of a molecule is described by vertices (atoms) and edges (bonds), called the molecular graph of a molecule, which in turn provides the total information contained in a molecule. Topological indices are a powerful tool [11–15] for predicting physical and thermodynamic properties, biological activities, pharmacological and toxicological properties of liquids and their mixtures. Such indices are derived from the molecular structure without any experimental input. In recent studies [16–20], we have employed Graph theory (which deals with the topology of a molecule) successfully to determine V^E , H^E , excess Gibbs energy G^E , and κ_S^E of binary and ternary organic liquid mixtures. It will be of interest to see how Graph theory describes the thermodynamic properties of ionic liquid mixtures. A literature survey has revealed thermodynamic data have not been reported for 1-ethyl-3-methylimidazolium tetrafluoroborate (1) + *N*-methyl formamide or *N,N*-dimethyl formamide (2) mixtures. Consequently, we report here new ρ and u data of 1-ethyl-3-methylimidazolium tetrafluoroborate (1) + *N*-methyl formamide or *N,N*-dimethyl formamide (2) mixtures at (293.15, 298.15, 303.15 and 308.15) K and H^E data of the same mixtures at 298.15 K over entire composition range.

2 Experimental

1-Ethyl-3-methylimidazolium tetrafluoroborate [emim][BF₄] (Fluka, 0.98 GC) was used without further purification. The water content in this ionic liquid was regularly checked using Karl Fischer titrations [21] and the content of water was observed to be 350 ppm. *N*-methylformamide (NMF) (Fluka, >0.98 GC) was shaken with sodium hydroxide pellets and barium oxide for at least 4 h, filtered, and the filtrate was distilled under reduced pressure. The middle fraction was collected and stored in small bottles over anhydrous calcium chloride in a desiccator [22]. *N,N*-dimethylformamide (DMF) (Fluka, >0.98 GC) was distilled with benzene at atmospheric pressure and the water–benzene azeotrope was collected (which distills between 70 and 75 °C); the residual solution was shaken with powdered barium oxide, filtered and distilled under nitrogen at reduced pressure [23]. The purities of the purified liquids were checked by measuring their density and speed of sound values. The ρ and u values for the purified liquids (recorded in Table 1) compare well with their corresponding literature values [22, 24–32].

The ρ and u values of the pure liquids and their binary mixtures were measured at the desired temperatures using a density and sound analyzer (Anton Paar DSA 5000) in the manner described elsewhere [33, 34]. The apparatus was calibrated with double distilled, deionized and degassed water. The mole fraction of each mixture was determined from the

Table 1 Comparison of densities, ρ , speeds of sound, u , and heat capacities, C_p , of pure liquids with their literature values at $T = (293.15, 298.15, 303.15, 308.15)$ K

Liquids	T/K	$\rho/\text{kg}\cdot\text{m}^{-3}$		$u/\text{m}\cdot\text{s}^{-1}$		$C_p/\text{J}\cdot\text{K}^{-1}\cdot\text{mol}^{-1}$
		Expt.	Lit.	Expt.	Lit.	
1-Ethyl-3-methyl imidazolium tetrafluoro borate	293.15	1283.89	1284.30 [24]	1631.05	–	303.2 [37]
	298.15	1279.91	1279.60 [25]	1619.40	–	304.9 [37]
			1280.07 [26]			
	303.15	1276.26	1276.50 [24]	1607.63	–	306.6 [37]
1275.70 [25]						
308.15	1272.07	1271.90 [25]	1596.31	–	308.4 [37]	
<i>N</i> -Methyl formamide	293.15	1003.35	–	1446.37	–	–
	298.15	999.007	999.00 [27]	1431.89	1431.5 [32]	124.0 [38]
			999.06 [28]			
	303.15	994.656	–	1417.68	–	125.1
308.15	990.305	–	1402.59	–	126.2	
<i>N,N</i> -Dimethyl formamide	293.15	948.735	944.50 [29]	1477.81	–	147.1 [29]
			949.17 [29]			
	298.15	944.608	944.60 [28]	1458.59	1458.5 [32]	148.3 [22]
	303.15	939.839	939.376 [30]	1440.32	–	150.2 [39]
940.691 [31]						
308.15	935.054	934.402 [30]	1420.95	–	152.3 [39]	
			935.814 [31]			

measured apparent masses of the components. All of the measurements were performed on an electronic balance. The uncertainties in mole fraction are 1×10^{-4} . The uncertainties in the density and speed of sound measurements are $2 \times 10^{-3} \text{ kg}\cdot\text{m}^{-3}$ and $0.1 \text{ m}\cdot\text{s}^{-1}$ respectively. The uncertainty in V^E values predicted from density results is 0.1 %. Also, the uncertainty in the temperature measurement is ± 0.01 K.

Values of H^E for the studied mixtures were measured with a 2-drop calorimeter (model, 4600) supplied by the Calorimeter Sciences Corporation (CSC), USA, at 298.15 K. The 2-drop calorimeter consists of a reaction vessel, a rapidly responding thermoelectric device (TED) as the heat measuring sensor, an electric heater for calibration, and a burette system for titrant addition. The heat flow between the reaction vessel and the constant temperature block was detected by the TED sensor, amplified, and then converted from an analogue signal to a digital signal in the data collection system. The temperature of the constant temperature block was actively controlled using the block control TEDs. The amounts of liquids in the micro syringe and vial (in CSA 2-Drop Calorimeter) for enthalpy measurements were determined by weight and the uncertainty in mole fraction in enthalpy measurement is 1×10^{-4} . The H^E values of the present mixtures were measured in the manner described elsewhere [35]. The uncertainties in the measured H^E values are 1 %.

The equimolar liquid mixtures were prepared by mixing (1) and (2) components in a 1:1 (mol/mol) ratio. Spectra of the samples were recorded by a Perkin Elmer Spectrum RX-1, FTIR spectrometer.

3 Results

The experimental values of ρ_{12} and u_{12} of [emim][BF₄] with NMF or DMF at (293.15, 298.15, 303.15 and 308.15) K, and H_{12}^E at 298.15 K, over the entire range of composition at atmospheric pressure are presented, respectively, in Tables 2 and 3. The V_{12}^E and $(\kappa_S)_{12}$ values for the studied mixtures were determined from density and speed of sound values using:

$$V_{12}^E = \sum_{i=1}^2 x_i M_i (\rho_{12})^{-1} - \sum_{i=1}^2 x_i M_i (\rho_i)^{-1} \quad (1)$$

$$(\kappa_S)_{12} = (\rho_{12} u_{12}^2)^{-1} \quad (2)$$

where x_i , M_i and ρ_i are the mole fraction, molar mass and density of [emim][BF₄] and ρ_{12} is the density of the (1 + 2) mixture. The $(\kappa_S^E)_{12}$ values were then determined by using

$$\kappa_S^E = \kappa_S - \kappa_S^{\text{id}} \quad (3)$$

The κ_S^{id} values were evaluated by employing the following relation [36]

$$\kappa_S^{\text{id}} = \sum_{i=1}^2 \phi_i \left[\kappa_{s,i} + \frac{T v_i \alpha_i^2}{C_{p,i}} \right] - T \left(\sum_{i=1}^2 x_i v_i \right) \frac{\left(\sum_{i=1}^2 \phi_i \alpha_i \right)^2}{\left(\sum_{i=1}^2 x_i C_{p,i} \right)} \quad (4)$$

where ϕ_i is the volume fraction of component (1). The $\kappa_{s,i}$, v_i , α_i and $C_{p,i}$ are isentropic compressibility, molar volume, thermal expansion coefficient, and molar heat capacity, respectively, of the pure component (1). The C_p values for the investigated liquids were taken from the literature [22, 29, 37–39] and are reported in Table 1. While the α values for [emim][BF₄] were predicted by using experimental density data in the manner described elsewhere [40], those for NMF and DMF were taken from the literature [28]. The $(\kappa_S^E)_{12}$ values for the (1 + 2) mixtures are recorded in Table 2.

The V_{12}^E , H_{12}^E and $(\kappa_S^E)_{12}$ values (plotted in Figs. 1, 2, 3, 4, 5, 6, 7, 8, 9) were fitted with the Redlich–Kister equation, Eq. 5:

$$Y_{12}^E (Y = V \text{ or } H \text{ or } \kappa_S) = x_1 x_2 [Y^{(0)} + Y^{(1)}(2x_1 - 1) + Y^{(2)}(2x_2 - 1)^2] \quad (5)$$

where $Y_{12}^{(n)}$ ($n = 0 - 2$), etc., are binary adjustable parameters and were determined by fitting Y_{12}^E ($Y = V \text{ or } H \text{ or } \kappa_S$) data to Eq. 5 using the least-squares method. The parameters along with their standard deviations, $\sigma(Y_{12}^E)$ ($Y = V \text{ or } H \text{ or } \kappa_S$), are listed in Table 4.

4 Discussion

The V_{12}^E and $(\kappa_S^E)_{12}$ values for the (1 + 2) mixtures are negative over the entire composition range and for the equimolar composition follow the sequence: NMF > DMF. However, while the H_{12}^E values for the [emim][BF₄] (1) + DMF (2) mixtures are negative,

Table 2 Measured densities, ρ_{12} , excess molar volumes, V_{12}^E , speeds of sound, u_{12} , isentropic compressibilities, $(\kappa_S)_{12}$, and excess isentropic compressibilities, $(\kappa_S^E)_{12}$, for the various (1 + 2) mixtures as a function of mole fraction, x_1 , of component (1) at $T = (293.15, 298.15, 303.15, 308.15)$ K

x_1	$\rho_{12}/(\text{kg}\cdot\text{m}^{-3})$	$V_{12}^E/(\text{cm}^3\cdot\text{mol}^{-1})$	$u_{12}/(\text{m}\cdot\text{s}^{-1})$	$(\kappa_S)_{12}/(\text{TPa}^{-1})$	$(\kappa_S^E)_{12}/(\text{TPa}^{-1})$
1-Ethyl-3-methylimidazolium tetrafluoroborate (1) + <i>N</i> -methylformamide (2)					
$T = 293.15$ K					
0.1218	1,084.52	-0.412	1467.7	428.1	-26.0
0.1729	1,110.66	-0.540	1481.1	410.5	-34.2
0.2256	1,133.96	-0.645	1496.7	393.7	-41.3
0.2719	1,151.94	-0.719	1511.5	380.0	-46.5
0.3227	1,169.36	-0.780	1527.6	366.5	-50.7
0.3748	1,185.09	-0.819	1543.5	354.2	-53.4
0.4251	1,198.57	-0.839	1559.2	343.2	-55.2
0.4709	1,209.60	-0.845	1572.2	334.5	-55.5
0.5234	1,220.92	-0.831	1585.5	325.8	-54.5
0.5741	1,230.75	-0.804	1597.9	318.2	-52.8
0.6271	1,239.97	-0.759	1608.1	311.9	-49.4
0.6713	1,246.92	-0.706	1616.2	307.0	-46.1
0.7217	1,254.19	-0.637	1622.6	302.8	-41.0
0.7742	1,261.03	-0.549	1628.0	299.2	-35.0
0.8243	1,266.95	-0.449	1631.7	296.5	-28.6
0.8713	1,272.03	-0.346	1633.0	294.8	-21.6
0.9114	1,276.03	-0.247	1633.3	293.8	-15.3
0.9339	1,278.15	-0.189	1633.3	293.3	-11.6
$T = 298.15$ K					
0.1218	1,080.14	-0.411	1453.9	438.0	-27.1
0.1729	1,106.34	-0.543	1467.1	420.0	-35.4
0.2256	1,129.78	-0.657	1482.3	402.9	-42.5
0.2719	1,147.84	-0.736	1496.7	388.9	-47.6
0.3227	1,165.33	-0.801	1511.9	375.4	-51.4
0.3748	1,181.16	-0.847	1527.8	362.7	-54.2
0.4251	1,194.73	-0.874	1543.2	351.5	-55.9
0.4709	1,205.75	-0.877	1556.2	342.5	-56.1
0.5234	1,217.12	-0.867	1569.5	333.6	-55.1
0.5741	1,226.91	-0.836	1582.3	325.6	-53.4
0.6271	1,236.10	-0.786	1593.0	318.8	-50.1
0.6713	1,243.06	-0.733	1601.7	313.6	-46.9
0.7217	1,250.27	-0.656	1609.0	308.9	-42.0
0.7742	1,257.05	-0.559	1615.8	304.7	-36.2
0.8243	1,262.95	-0.456	1619.5	301.9	-29.5
0.8713	1,268.00	-0.346	1622.1	299.7	-22.7
0.9114	1,272.00	-0.246	1622.4	298.7	-16.1
0.9339	1,274.11	-0.186	1622.4	298.2	-12.3
$T = 303.15$ K					
0.1218	1,076.24	-0.437	1439.9	448.1	-28.1
0.1729	1,102.50	-0.572	1453.0	429.6	-36.5

Table 2 continued

x_1	$\rho_{12}/(\text{kg}\cdot\text{m}^{-3})$	$V_{12}^E/(\text{cm}^3\cdot\text{mol}^{-1})$	$u_{12}/(\text{m}\cdot\text{s}^{-1})$	$(\kappa_S)_{12}/(\text{TPa}^{-1})$	$(\kappa_S^E)_{12}/(\text{TPa}^{-1})$
0.2256	1,125.95	-0.684	1467.9	412.2	-43.6
0.2719	1,144.03	-0.764	1482.0	398.0	-48.7
0.3227	1,161.54	-0.828	1496.9	384.2	-52.4
0.3748	1,177.36	-0.870	1513.0	371.0	-55.4
0.4251	1,190.94	-0.895	1527.8	359.7	-56.7
0.4709	1,201.97	-0.898	1540.2	350.7	-56.7
0.5234	1,213.36	-0.886	1554.2	341.2	-55.9
0.5741	1,223.23	-0.859	1567.3	332.8	-54.3
0.6271	1,232.47	-0.811	1579.1	325.4	-51.3
0.6713	1,239.44	-0.757	1587.3	320.2	-47.7
0.7217	1,246.69	-0.682	1595.9	315.0	-43.1
0.7742	1,253.53	-0.588	1603.3	310.3	-37.4
0.8243	1,259.46	-0.485	1607.8	307.2	-30.6
0.8713	1,264.51	-0.373	1610.8	304.8	-23.7
0.9114	1,268.49	-0.268	1611.3	303.6	-17.0
0.9339	1,270.59	-0.205	1611.3	303.2	-13.0
$T = 308.15 \text{ K}$					
0.1218	1,071.89	-0.442	1424.2	460.0	-28.4
0.1729	1,098.22	-0.582	1437.0	440.9	-37.0
0.2256	1,121.76	-0.702	1452.1	422.8	-44.3
0.2719	1,139.86	-0.783	1465.8	408.3	-49.3
0.3227	1,157.45	-0.854	1480.7	394.1	-53.2
0.3748	1,173.34	-0.902	1496.9	380.4	-56.2
0.4251	1,186.90	-0.925	1511.9	368.6	-57.7
0.4709	1,197.98	-0.931	1524.6	359.1	-57.8
0.5234	1,209.37	-0.919	1539.1	349.1	-57.0
0.5741	1,219.22	-0.891	1552.1	340.5	-55.3
0.6271	1,228.44	-0.840	1565.1	332.3	-52.6
0.6713	1,235.39	-0.782	1573.9	326.8	-49.0
0.7217	1,242.62	-0.705	1583.5	321.0	-44.6
0.7742	1,249.42	-0.606	1590.7	316.3	-38.5
0.8243	1,255.30	-0.496	1596.1	312.7	-31.8
0.8713	1,260.32	-0.379	1599.4	310.2	-24.7
0.9114	1,264.28	-0.270	1600.3	308.8	-17.8
0.9339	1,266.39	-0.206	1600.0	308.5	-13.6
$1\text{-Ethyl-3-methylimidazolium tetrafluoroborate (1) + }N,N\text{-dimethylformamide (2)}$					
$T = 293.15 \text{ K}$					
0.1211	1,032.20	-0.915	1513.1	423.2	-36.5
0.1732	1,062.06	-1.209	1529.4	402.6	-47.2
0.2310	1,091.66	-1.474	1546.4	383.1	-55.7
0.2709	1,110.19	-1.622	1558.1	371.0	-60.2
0.3242	1,132.68	-1.770	1572.0	357.3	-63.8
0.3739	1,151.55	-1.858	1582.9	346.6	-65.1

Table 2 continued

x_1	$\rho_{12}/(\text{kg}\cdot\text{m}^{-3})$	$V_{12}^E/(\text{cm}^3\cdot\text{mol}^{-1})$	$u_{12}/(\text{m}\cdot\text{s}^{-1})$	$(\kappa_S)_{12}/(\text{TPa}^{-1})$	$(\kappa_S^E)_{12}/(\text{TPa}^{-1})$
0.4303	1,170.92	-1.916	1593.8	336.2	-64.7
0.4742	1,184.50	-1.917	1600.8	329.4	-63.2
0.5243	1,198.74	-1.891	1607.8	322.7	-60.4
0.5773	1,212.33	-1.817	1612.9	317.1	-56.0
0.6219	1,222.73	-1.722	1615.6	313.3	-51.2
0.6724	1,233.56	-1.589	1618.1	309.6	-45.4
0.7219	1,243.17	-1.421	1620.2	306.4	-39.2
0.7725	1,252.15	-1.222	1621.4	303.8	-32.2
0.8283	1,261.17	-0.972	1622.4	301.2	-24.1
0.8743	1,267.94	-0.739	1623.9	299.1	-17.6
0.9097	1,272.78	-0.544	1625.1	297.5	-12.4
0.9319	1,275.68	-0.418	1626.2	296.4	-9.3
$T = 298.15 \text{ K}$					
0.1211	1,028.29	-0.943	1495.6	434.8	-38.7
0.1732	1,058.27	-1.251	1512.2	413.2	-49.8
0.2310	1,087.94	-1.524	1530.8	392.3	-59.2
0.2709	1,106.43	-1.670	1542.1	380.1	-63.5
0.3242	1,128.95	-1.822	1556.4	365.7	-67.2
0.3739	1,147.93	-1.920	1568.1	354.3	-68.7
0.4303	1,167.23	-1.971	1579.9	343.2	-68.5
0.4742	1,180.91	-1.982	1586.4	336.5	-66.5
0.5243	1,195.07	-1.947	1593.5	329.6	-63.4
0.5773	1,208.67	-1.873	1598.5	323.8	-58.6
0.6219	1,219.13	-1.784	1601.0	320.0	-53.4
0.6724	1,229.91	-1.645	1603.9	316.1	-47.3
0.7219	1,239.50	-1.473	1605.5	313.0	-40.5
0.7725	1,248.46	-1.269	1606.7	310.3	-33.1
0.8283	1,257.44	-1.011	1607.9	307.6	-24.6
0.8743	1,264.14	-0.769	1609.6	305.3	-17.7
0.9097	1,268.96	-0.570	1611.5	303.4	-12.5
0.9319	1,271.81	-0.436	1612.9	302.3	-9.3
$T = 303.15 \text{ K}$					
0.1211	1,023.91	-0.975	1478.4	446.9	-40.7
0.1732	1,053.99	-1.289	1495.4	424.3	-52.3
0.2310	1,083.75	-1.565	1513.9	402.6	-61.9
0.2709	1,102.28	-1.712	1526.5	389.3	-66.8
0.3242	1,124.85	-1.864	1541.3	374.2	-70.7
0.3739	1,143.89	-1.962	1552.6	362.6	-71.9
0.4303	1,163.29	-2.017	1564.7	351.1	-71.6
0.4742	1,176.93	-2.019	1571.3	344.1	-69.3
0.5243	1,191.20	-1.989	1577.9	337.2	-65.8
0.5773	1,204.87	-1.916	1583.6	330.9	-60.9
0.6219	1,215.39	-1.827	1586.1	327.1	-55.4

Table 2 continued

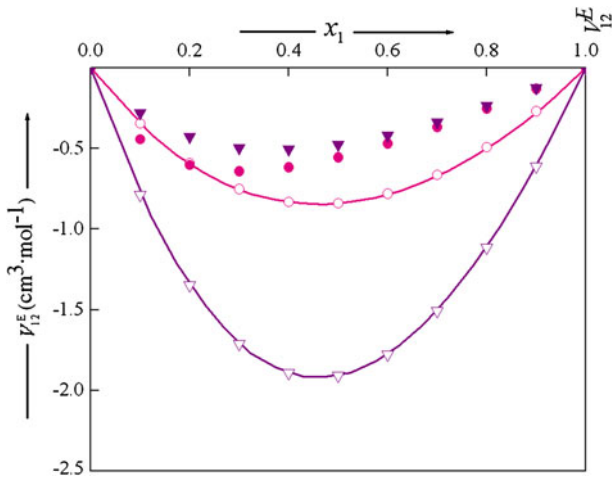
x_1	$\rho_{12}/(\text{kg}\cdot\text{m}^{-3})$	$V_{12}^E/(\text{cm}^3\cdot\text{mol}^{-1})$	$u_{12}/(\text{m}\cdot\text{s}^{-1})$	$(\kappa_S)_{12}/(\text{TPa}^{-1})$	$(\kappa_S^E)_{12}/(\text{TPa}^{-1})$
0.6724	1,226.21	-1.685	1589.2	322.9	-49.0
0.7219	1,235.92	-1.520	1590.4	319.9	-41.6
0.7725	1,244.93	-1.314	1591.9	317.0	-33.9
0.8283	1,253.90	-1.048	1594.0	313.9	-25.3
0.8743	1,260.63	-0.802	1596.0	311.4	-18.1
0.9097	1,265.42	-0.596	1598.0	309.5	-12.7
0.9319	1,268.27	-0.459	1599.8	308.1	-9.4
$T = 308.15 \text{ K}$					
0.1211	1,019.61	-1.023	1460.1	460.1	-42.8
0.1732	1,049.83	-1.350	1478.0	436.1	-55.3
0.2310	1,079.77	-1.644	1496.7	413.5	-65.2
0.2709	1,098.50	-1.807	1508.1	400.3	-69.5
0.3242	1,121.21	-1.971	1523.2	384.4	-73.6
0.3739	1,140.24	-2.068	1534.5	372.4	-74.6
0.4303	1,159.71	-2.127	1546.5	360.5	-74.0
0.4742	1,173.46	-2.138	1553.1	353.3	-71.5
0.5243	1,187.72	-2.105	1560.5	345.8	-68.0
0.5773	1,201.32	-2.022	1565.4	339.7	-62.3
0.6219	1,211.75	-1.922	1569.6	335.0	-57.2
0.6724	1,222.57	-1.777	1572.2	330.9	-50.1
0.7219	1,232.13	-1.593	1574.8	327.3	-42.8
0.7725	1,241.05	-1.374	1577.6	323.8	-35.1
0.8283	1,249.96	-1.097	1580.1	320.4	-26.0
0.8743	1,256.59	-0.835	1583.1	317.6	-18.8
0.9097	1,261.34	-0.619	1586.0	315.2	-13.3
0.9319	1,264.14	-0.474	1588.0	313.7	-9.9

those for [emim][BF₄] (1) + NMF (2) mixtures are positive over the entire composition range.

The H_{12}^E data of the studied mixtures may be explained qualitatively, if it is assumed that (i) [emim][BF₄] is characterized by ionic interactions and exists as its monomer, while NMF and DMF exist as associated entities and there is formation of 1–2_n contacts in the mixed state; (ii) unlike 1–2_n contacts lead to weakening of ionic interactions and also rupture of the associated amide molecules to form their respective monomers; and (iii) ion–dipole interactions (between the N atom of the imidazolium ring and the fluorine atom of the [BF₄][−] anion with the oxygen atom of NMF or DMF and the hydrogen atom of NMF) exist in the mixtures. The H_{12}^E values for [emim][BF₄] (1) + DMF (2) mixtures suggest that the contribution to H_{12}^E due to factors (i) and (iii) outweigh the contribution to H_{12}^E due to factor (ii), and thus the overall H_{12}^E values for this mixture are negative. Further, amide–amide interactions become weaker in the sequence primary > secondary > tertiary, so the contribution to H_{12}^E due to rupture of NMF–NMF interactions upon mixing will be larger than that related to the breaking of DMF–DMF interactions, and consequently the

Table 3 Measured excess molar enthalpy, H_{12}^E , values for the various (1 + 2) mixtures as a function of mole fraction x_1 , of component (1) at 298.15 K

x_1	$H_{12}^E/(\text{J}\cdot\text{mol}^{-1})$	x_1	$H_{12}^E/(\text{J}\cdot\text{mol}^{-1})$
1-Ethyl-3-methylimidazolium tetrafluoroborate (1) + <i>N</i> -methylformamide (2)			
0.1241	193	0.5136	481
0.1688	249	0.5687	479
0.2013	294	0.6022	469
0.2597	358	0.6648	434
0.2991	394	0.7112	397
0.3346	425	0.7732	339
0.3875	455	0.8453	245
0.4221	470	0.8951	177
0.4793	479	0.9156	143
1-Ethyl-3-methylimidazolium tetrafluoroborate (1) + <i>N,N</i> -dimethylformamide (2)			
0.1004	-260	0.5561	-912
0.1532	-386	0.5945	-905
0.1962	-483	0.6687	-849
0.2565	-611	0.7148	-803
0.3285	-725	0.7851	-674
0.3798	-803	0.8257	-590
0.4155	-842	0.8711	-461
0.4621	-879	0.8991	-381
0.5021	-894	0.9156	-322

**Fig. 1** Excess molar volumes, V_{12}^E , at $T = 293.15$ for: (I) 1-ethyl-3-methylimidazolium tetrafluoroborate (1) + *N*-methyl formamide (2). The line represents fitting of the measured data with Eq. 5, pink curved line, Graph pink open circle, PFP pink filled circle. (II) 1-Ethyl-3-methylimidazolium tetrafluoroborate (1) + *N,N*-dimethyl formamide (2). The line represents fitting of the measured data with Eq. 5, violet curved line, Graph violet down-pointing open triangle, PFP violet down-pointing filled triangle

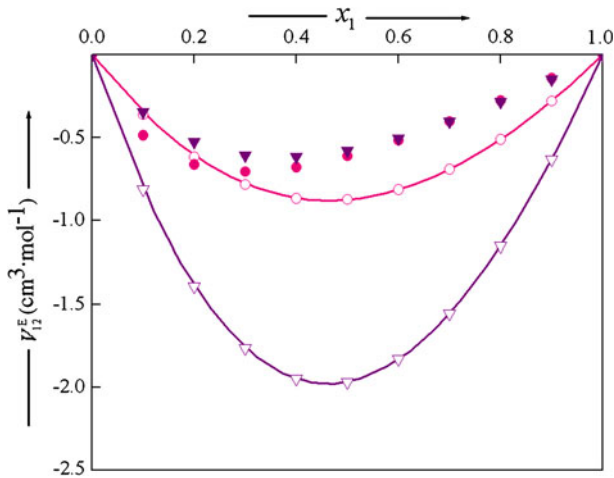


Fig. 2 Excess molar volumes, V_{12}^E , at $T = 298.15$ for: (I) 1-ethyl-3-methylimidazolium tetrafluoroborate (1) + *N*-methyl formamide (2). The line represents fitting of the measured data with Eq. 5, pink curved line, Graph pink open circle, PFP pink filled circle. (II) 1-Ethyl-3-methylimidazolium tetrafluoroborate (1) + *N,N*-dimethyl formamide (2). The line represents fitting of the measured data with Eq. 5, violet curved line, Graph violet down-pointing open triangle, PFP violet down-pointing filled triangle

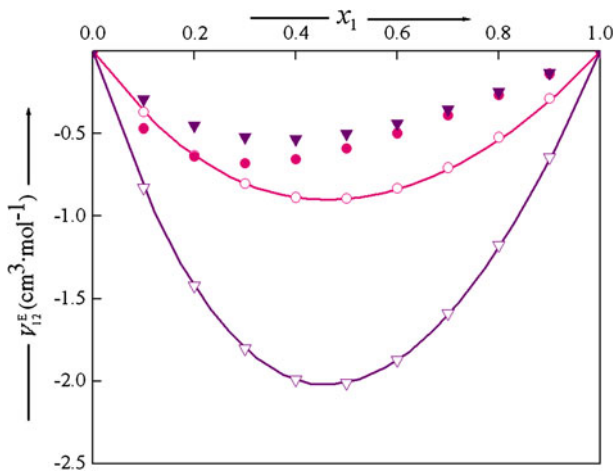


Fig. 3 Excess molar volumes, V_{12}^E , at $T = 303.15$ for: (I) 1-ethyl-3-methylimidazolium tetrafluoroborate (1) + *N*-methyl formamide (2). The line represents fitting of the measured data with Eq. 5, pink curved line, Graph pink open circle, PFP pink filled circle. (II) 1-Ethyl-3-methylimidazolium tetrafluoroborate (1) + *N,N*-dimethyl formamide (2). The line represents fitting of the measured data with Eq. 5, violet curved line, Graph violet down-pointing open triangle, PFP violet down-pointing filled triangle

contribution to H_{12}^E from factor (ii) will outweigh the contribution due to factors (ii) and (iii), which leads to the positive values of H_{12}^E for [emim][BF₄] (1) + NMF (2) mixtures.

The sign as well as the magnitude of V_{12}^E and $(\kappa_S^E)_{12}$ arise due to (i) rupture of associated entities in the mixed state, to (ii) the molecular arrangement and packing of the constituents of mixtures, and (iii) molecular interactions existing in these mixtures. The negative V_{12}^E values for these mixtures suggest that the contribution to V_{12}^E due to ion—the dipole

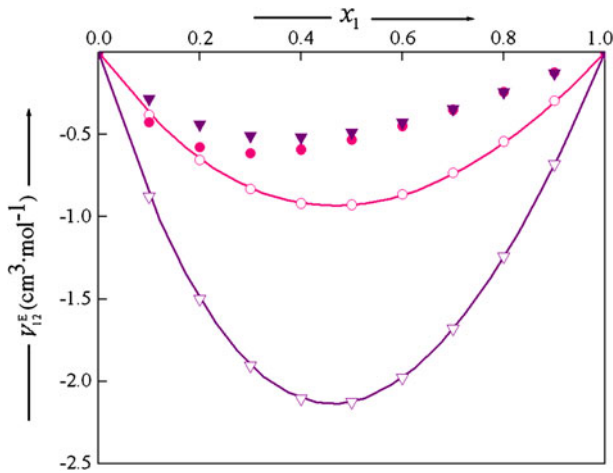


Fig. 4 Excess molar volumes, V_{12}^E , at $T = 308.15$ for (I) 1-ethyl-3-methylimidazolium tetrafluoroborate (1) + *N*-methyl formamide (2). The line represents fitting of the measured data with Eq. 5, pink curved line, Graph pink open circle, PFP pink filled circle. (II) 1-Ethyl-3-methylimidazolium tetrafluoroborate (1) + *N,N*-dimethyl formamide (2). The line represents fitting of the measured data with Eq. 5, violet curved line, Graph violet down-pointing open triangle, PFP violet down-pointing filled triangle

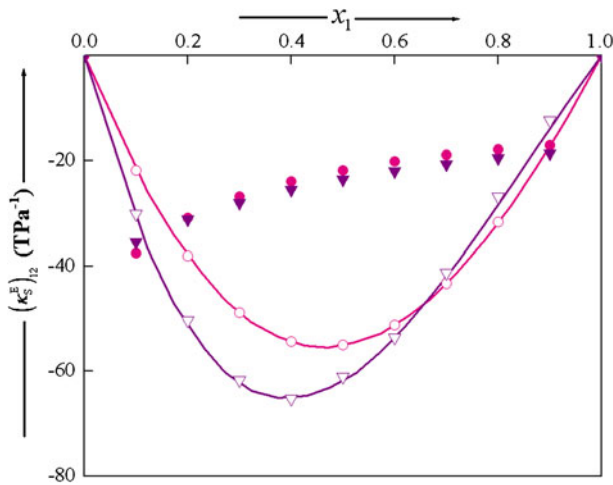


Fig. 5 Excess isentropic compressibilities, $(\kappa_S^E)_{12}$, at $T = 293.15$ for (I) 1-ethyl-3-methylimidazolium tetrafluoroborate (1) + *N*-methyl formamide (2). The line represents fitting of the measured data with Eq. 5, pink curved line, Graph pink open circle, PFP pink filled circle. (II) 1-Ethyl-3-methylimidazolium tetrafluoroborate (1) + *N,N*-dimethyl formamide (2). The line represents fitting of the measured data with Eq. 5, violet curved line, Graph violet down-pointing open triangle, PFP violet down-pointing filled triangle

interactions and molecular packing is more than that of the contribution from rupture of associated entities. This may be due to (i) the larger difference between the molar volumes of [emim][BF₄] ($154.70 \times 10^{-6} \text{ m}^3 \cdot \text{mol}^{-1}$) and NMF ($59.06 \times 10^{-6} \text{ m}^3 \cdot \text{mol}^{-1}$) or DMF ($77.28 \times 10^{-6} \text{ m}^3 \cdot \text{mol}^{-1}$), which allows small molecules to fit into the available free volume of the ionic liquid; and (ii) ion–dipole interactions occur in the mixtures. Further,

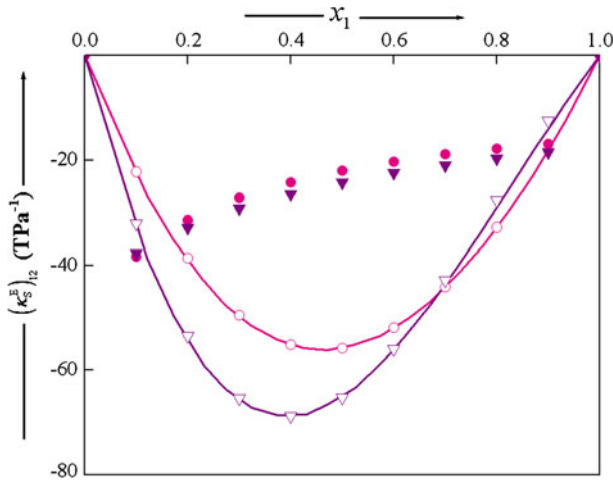


Fig. 6 Excess isentropic compressibilities, $(\kappa_S^E)_{12}$, at $T = 298.15$ for (I) 1-ethyl-3-methylimidazolium tetrafluoroborate (1) + *N*-methyl formamide (2). The line represents fitting of the measured data with Eq. 5, pink curved line, Graph pink open circle, PFP pink filled circle. (II) 1-Ethyl-3-methylimidazolium tetrafluoroborate (1) + *N,N*-dimethyl formamide (2). The line represents fitting of the measured data with Eq. 5, violet curved line, Graph violet down-pointing open triangle, PFP violet down-pointing filled triangle

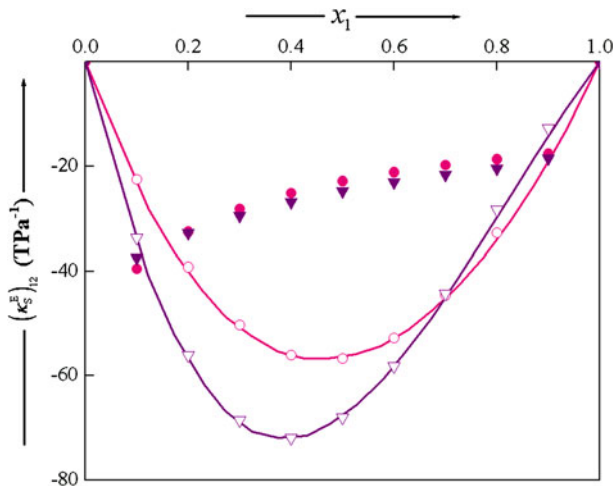


Fig. 7 Excess isentropic compressibilities, $(\kappa_S^E)_{12}$, at $T = 303.15$ for (I) 1-ethyl-3-methylimidazolium tetrafluoroborate (1) + *N*-methyl formamide (2). The line represents fitting of the measured data with Eq. 5, pink curved line, Graph pink open circle, PFP pink filled circle. (II) 1-Ethyl-3-methylimidazolium tetrafluoroborate (1) + *N,N*-dimethyl formamide (2). The line represents fitting of the measured data with Eq. 5, violet curved line, Graph violet down-pointing open triangle, PFP violet down-pointing filled triangle

the V_{12}^E values suggest that (1 + 2) mixtures contain relatively more packed structure in the mixed state as compared to their pure states. The temperature coefficients $(\partial V^E/\partial T)$ and $(\partial \kappa_S^E/\partial T)$ are negative for the studied mixtures, which in turn suggests that the ion–dipole interaction increases with rise in temperature. The decrease in speed of sound values for the mixtures with increasing temperature also supports this viewpoint.

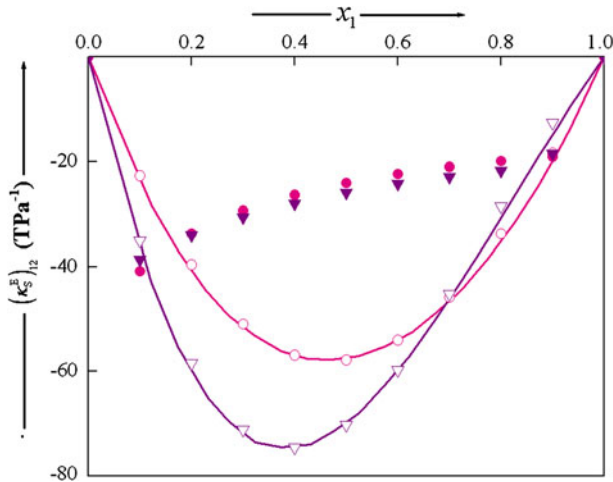


Fig. 8 Excess isentropic compressibilities, $(\kappa_S^E)_{12}$, at $T = 308.15$ for (I) 1-ethyl-3-methylimidazolium tetrafluoroborate (1) + *N*-methyl formamide (2). The line represents fitting of the measured data with Eq. 5, pink curved line, Graph pink open circle, PFP pink filled circle. (II) 1-Ethyl-3-methylimidazolium tetrafluoroborate (1) + *N,N*-dimethyl formamide (2). The line represents fitting of the measured data with Eq. 5, violet curved line, Graph violet down-pointing open triangle, PFP violet down-pointing filled triangle

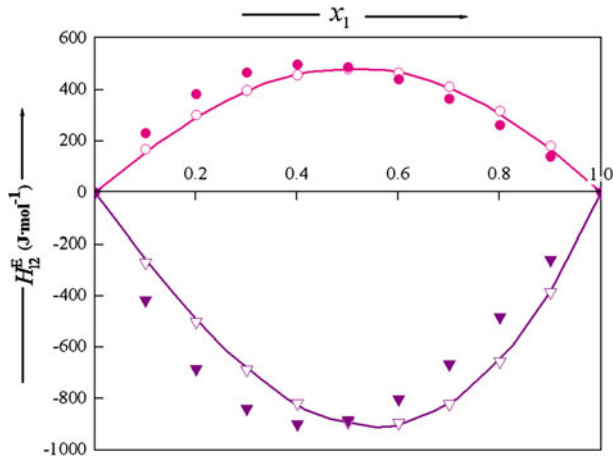


Fig. 9 Excess molar enthalpies, H_{12}^E , at $T = 298.15$ for (I) 1-ethyl-3-methylimidazolium tetrafluoroborate (1) + *N*-methyl formamide (2). The line represents fitting of the measured data with Eq. 5, pink curved line, Graph pink open circle, PFP pink filled circle. (II) 1-Ethyl-3-methylimidazolium tetrafluoroborate (1) + *N,N*-dimethyl formamide (2). The line represents fitting of the measured data with Eq. 5, violet curved line, Graph violet down-pointing open triangle, PFP violet down-pointing filled triangle

5 Graph Theory

5.1 Excess Molar Volumes

Graph theory deals with the topology of molecules constituting the mixture. As the topology of the molecules changes on addition of component 1–2 or vice versa, it is,

Table 4 Binary adjustable parameters $V_{12}^E(Y = V \text{ or } H \text{ or } \kappa_S)$, $n = 0-2$ of Eq. 5, along with their corresponding standard deviations, $\sigma(Y_{12}^E)$ of V_{12}^E, H_{12}^E and $(\kappa_S^E)_{12}$ at $T = (293.15, 298.15, 303.15, \text{ and } 308.15)$ K

Parameters	T/K			
	293.15	298.15	303.15	308.15
1-Ethyl-3-methylimidazolium tetrafluoroborate (1) + N-methylformamide (2)				
$V^{(0)}$	-3.358	-3.497	-3.580	-3.713
$V^{(1)}$	0.511	0.502	0.502	0.502
$V^{(2)}$	-0.188	0.061	-0.217	-0.075
$\sigma(V^E)/\text{cm}^3 \cdot \text{mol}^{-1}$	0.001	0.001	0.001	0.001
$\kappa_S^{(0)}$	-220.4	-222.9	-226.2	-230.5
$\kappa_S^{(1)}$	32.9	33.7	33.7	30.0
$\kappa_S^{(2)}$	5.0	-7.2	-18.3	-21.1
$\sigma(\kappa_S^E)/\text{TPa}^{-1}$	0.1	0.1	0.1	0.1
$H^{(0)}$	-	1,928	-	-
$H^{(1)}$	-	80	-	-
$H^{(2)}$	-	-193	-	-
$\sigma(H^E)/\text{J} \cdot \text{mol}^{-1}$	-	4	-	-
1-Ethyl-3-methylimidazolium tetrafluoroborate (1) + N,N-dimethylformamide (2)				
$V^{(0)}$	-7.633	-7.874	-8.041	-8.496
$V^{(1)}$	1.241	1.241	1.232	1.327
$V^{(2)}$	-0.020	-0.102	-0.341	-0.177
$\sigma(V^E)/\text{cm}^3 \cdot \text{mol}^{-1}$	0.002	0.002	0.002	0.002
$\kappa_S^{(0)}$	-247.5	-260.1	-271.2	-279.4
$\kappa_S^{(1)}$	121.3	133.8	143.9	154.2
$\kappa_S^{(2)}$	-4.9	-2.5	-1.6	-12.4
$\sigma(\kappa_S^E)/\text{TPa}^{-1}$	0.1	0.1	0.1	0.1
$H^{(0)}$	-	-3,574	-	-
$H^{(1)}$	-	-794	-	-
$H^{(2)}$	-	55	-	-
$\sigma(H^E)/\text{J} \cdot \text{mol}^{-1}$	-	5	-	-

therefore, worthwhile to analyze the V_{12}^E data in terms of Graph theory. According to this theory, V_{12}^E is given [41] by:

$$V_{12}^E = \alpha_{12} \left\{ \left[\sum x_i ({}^3 \xi_i)_m \right]^{-1} - \sum x_i ({}^3 \xi_i)^{-1} \right\} \tag{6}$$

where α_{12} is a constant characteristic of the (1 + 2) mixtures. The $({}^3 \xi_i)$ and $({}^3 \xi_i)_m$ ($i = 1$ or 2) are the connectivity parameters of third degree of the components (1) and (2) in the pure and mixed state and are defined [42] by:

$${}^3 \xi = \sum_{m < n < o < p} \left(\delta_m^v \delta_n^v \delta_o^v \delta_p^v \right)^{-0.5} \tag{7}$$

where the δ_m^v etc. values have the same significance as described elsewhere [43]. The

evaluation of V_{12}^E from Eq. 6 requires knowledge of the connectivity parameters of third degree, $({}^3\xi_i)$ ($i = 1$ or 2) or $({}^3\xi_i)_m$ ($i = 1$ or 2), that are parameters of the components of mixtures in their pure and mixed state. In the present investigations, we have evaluated these parameters from the measured V_{12}^E data at one temperature and 1 mole fraction ($x_1 = 0.5$). The $({}^3\xi_i)$ or $({}^3\xi_i)_m$ ($i = 1$ or 2) values were then subsequently utilized to predict V_{12}^E at other mole fractions. Such V_{12}^E values are shown in Figs. 1, 2, 3, 4 and are compared with the corresponding experimental values. Also, the $({}^3\xi_i)$, $({}^3\xi_i)_m$ ($i = 1$ or 2), and α_{12} values are listed in Table 5. Examination of Figs. 1, 2, 3, 4 reveals that the $({}^3\xi_i)$ or $({}^3\xi_i)_m$ ($i = 1$ or 2) values reproduce the experimental V_{12}^E data reasonably well and hence $({}^3\xi_i)$ or $({}^3\xi_i)_m$ ($i = 1$ or 2) can be utilized to extract information about the state of 1 and 2 in the pure and mixed states.

A number of structures were proposed for [emim][BF₄], NMF and DMF, and their ${}^3\xi'$ values were determined (using Eq. 7) taking in consideration their molecular structure. The structure or combination of structures that yielded ${}^3\xi'$ values that are comparable with the ${}^3\xi$ values (Table 5) were considered to be a representative structure of that component. For the (1 + 2) mixtures, it was assumed that [emim][BF₄], NMF and DMF in their pure states exist as the molecular entities I, II–III, and IV–V, respectively (Scheme 1). The ${}^3\xi'$ value for molecular entity I was predicted by using the proposed structure of [emim][BF₄] based on IR, Raman spectra and quantum mechanics analysis [44–46]. The proposed structure suggest that (i) the [BF₄][−] anion is positioned over the imidazolium ring of the [emim]⁺ cation and has short contacts with H–C(2) as well as a proton of the –CH₃ group (in imidazolium ring); and (ii) ion-pair formation strongly influences three antisymmetric B–F stretching vibrations of the [BF₄][−] anion and out-of-plane, stretching vibrations of the H–C(2) moiety of the cation. The ${}^3\xi'$ values for molecular entities I–V were then calculated to be 1.639, 0.236, 0.947, 0.211, 0.809. The experimental ${}^3\xi$ values are 1.505 and 1.502, 1.096, 1.095 for [emim][BF₄], NMF, and DMF (Table 5), which suggests that while [emim][BF₄] exist as a monomer (molecular entity I, ${}^3\xi' = 1.639$), NMF (molecular entity III, ${}^3\xi' = 0.947$) and DMF (molecular entity V, ${}^3\xi' = 0.809$) exist as associated entities in their pure state. The state of components in (1 + 2) mixed solutions were then studied by predicting $({}^3\xi'_2)_m$ values of NMF or DMF in [emim][BF₄]. For this purpose, we assumed that [emim][BF₄] (1) + NMF or DMF (2) mixtures possessed molecular entities VI and VII, respectively.

In evaluating $({}^3\xi'_2)_m$ values for these molecular entities VI and VII, it was assumed that while molecular entity VI is characterized by interactions between the N atom (N-3) of [emim]⁺ as well as a fluorine atom of [BF₄][−] with oxygen and hydrogen atoms of NMF, molecular entity VII is characterized by interactions among the N atom (N-3) of [emim]⁺ as well as the fluorine atom of [BF₄][−] with the oxygen of DMF. The $({}^3\xi'_2)_m$ values for these molecular entities were then predicted to be 0.891 and 1.084, respectively. The experimental $({}^3\xi_2)_m$ values of 1.096 and 1.095 for [emim][BF₄] (1) + NMF or DMF (2) mixtures (Table 5) suggest that these mixtures contain molecular entities VI and VII. To substantiate the existence of molecular entities VI and VII, we analyzed the spectral data of pure [emim][BF₄], NMF, DMF and [emim][BF₄] (1) + NMF or DMF (2) equimolar mixtures. Analysis of the IR data revealed that while [emim][BF₄], NMF and DMF in their pure states show characteristic vibrations at 3,130 cm^{−1} (C–H vibrations), 524 cm^{−1} (B–F stretching), 1,672 and 1,670 cm^{−1} (C=O), 3,170 cm^{−1} (N–H) [47], the [emim][BF₄] (1) + NMF or DMF (2) mixtures showed characteristic vibrations at 3,156 and 3,162 cm^{−1} (C–H vibrations), 536 and 533 cm^{−1} (B–F stretching), 1,660 and 1,659 cm^{−1} (C=O), and 3,182 cm^{−1} (N–H), respectively. The IR studies thus suggest that addition of

Table 5 Interaction energies χ^* , χ'_{12} , etc. parameters of Eq. 9 along with connectivity parameters of the third degree of a molecule, $({}^3\xi_i)$ or $({}^3\xi_j)_m$ ($i = 1$ or 2), and α_{12} of Eq. 6 utilized in Graph theory for the determination of V_{12}^E , H_{12}^E and $(\kappa_S^E)_{12}$ at $T = (293.15, 298.15, 303.15, 308.15)$ K

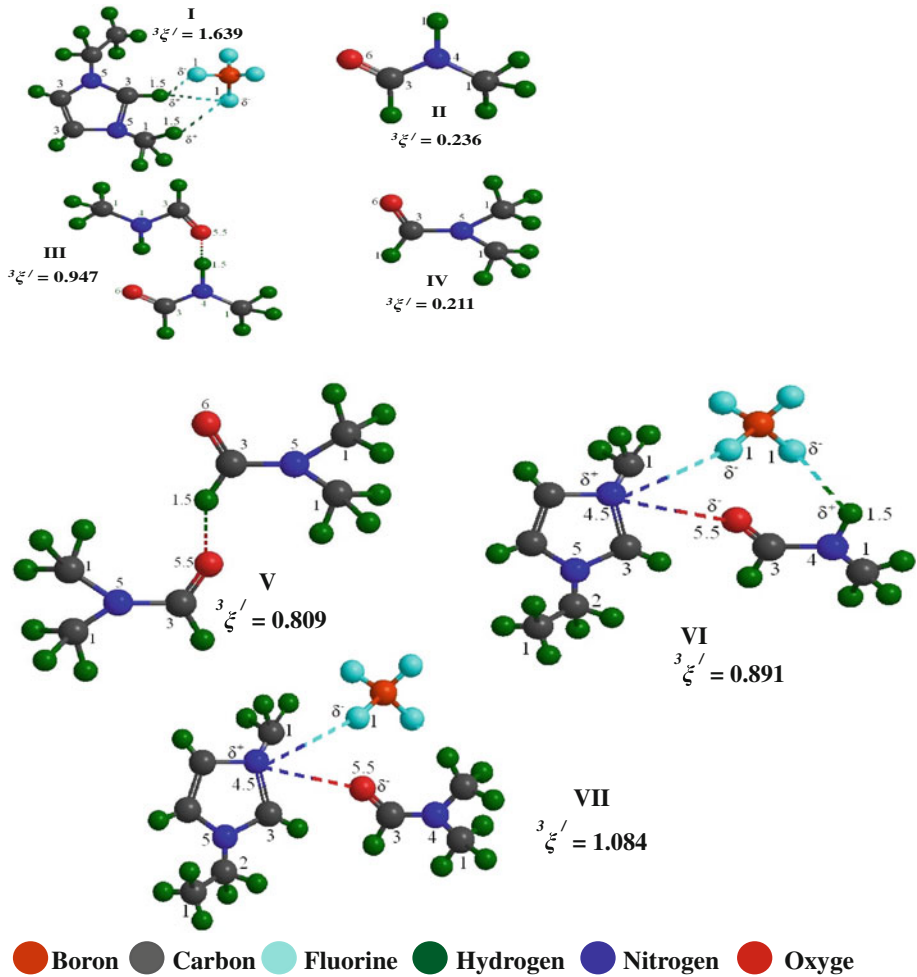
Parameters	T/K			
	293.15	298.15	303.15	308.15
1-Ethyl-3-methylimidazolium tetrafluoroborate (1) + <i>N</i> -methylformamide (2)				
$({}^3\xi_i) = ({}^3\xi_i)_m$	1.505	1.505	1.505	1.505
$({}^3\xi_j) = ({}^3\xi_j)_m$	1.096	1.096	1.096	1.096
$\alpha_{12}/\text{cm}^3\cdot\text{mol}^{-1}$	43.057	44.842	45.903	47.612
$\sigma(V^E, \text{Graph})$	0.005	0.008	0.008	0.007
χ^*/TPa^{-1}	-66.0	-66.8	-68.1	-71.4
$\chi'_{12}/\text{TPa}^{-1}$	-182.8	-185.6	-188.1	-186.1
$\sigma(\kappa_S^E, \text{Graph})$	1.1	0.5	1.0	1.1
$\chi^*/\text{J}\cdot\text{mol}^{-1}$	-	-733	-	-
$\chi'_{12}/\text{J}\cdot\text{mol}^{-1}$	-	-1116	-	-
$\sigma(H^E, \text{Graph})$	-	9	-	-
1-Ethyl-3-methylimidazolium tetrafluoroborate (1) + <i>N,N</i> -dimethylformamide (2)				
$({}^3\xi_i) = ({}^3\xi_i)_m$	1.503	1.503	1.503	1.503
$({}^3\xi_j) = ({}^3\xi_j)_m$	1.095	1.095	1.095	1.095
$\alpha_{12}/\text{cm}^3\cdot\text{mol}^{-1}$	98.022	101.130	103.267	109.118
$\sigma(V^E, \text{Graph})$	0.008	0.004	0.007	0.002
χ^*/TPa^{-1}	-38.1	-37.3	-37.0	-35.7
$\chi'_{12}/\text{TPa}^{-1}$	-315.1	-339.3	-359.3	-378.4
$\sigma(\kappa_S^E, \text{Graph})$	1.0	1.0	1.0	1.6
$\chi^*/\text{J}\cdot\text{mol}^{-1}$	-	-1642	-	-
$\chi'_{12}/\text{J}\cdot\text{mol}^{-1}$	-	-1239	-	-
$\sigma(H^E, \text{Graph})$	-	36	-	-

Also included are the standard deviations, $\sigma(V^E, \text{Graph})$, $\sigma(\kappa_S^E, \text{Graph})$, and $\sigma(H^E, \text{Graph})$ between experimental values, V_{12}^E , H_{12}^E and $(\kappa_S^E)_{12}$, and values obtained from Graph theory

NMF or DMF to $[\text{emim}][\text{BF}_4]$ does influence (i) the H–C(2) vibrations of $[\text{emim}]^+$, (ii) B–F stretching of $[\text{BF}_4]^-$, (iii) C=O vibrations of NMF or DMF, and (iv) N–H vibrations of NMF. Furthermore, shifting of the C–H vibrations to higher wave numbers suggest breaking of interactions between the hydrogen atom of the imidazolium ring of $[\text{emim}]^+$ and fluorine atom of $[\text{BF}_4]^-$, which in turn support the existence of molecular entities VI and VII in the studied mixtures.

5.2 Excess Molar Enthalpies and Excess Isentropic Compressibilities

The analysis of V_{12}^E data for the investigated mixtures in terms of Graph theory has revealed that while $[\text{emim}][\text{BF}_4]$ exists as a monomer, NMF and DMF exist as associated entities. The measured H_{12}^E and $(\kappa_S^E)_{12}$ data can be analyzed in terms of Graph theory, if it is assumed that the (1 + 2) investigated mixture formation involves the following processes: (i) formation of unlike 1– 2_n contacts; (ii) unlike contact formation then weakens 2_n – 2_n interactions and ionic interactions in $[\text{emim}][\text{BF}_4]$, which leads to the depolymerization of 2_n to



Scheme 1 Connectivity parameters, ${}^3\zeta'$ of the third degree for various molecular entities

form monomers of 2 components; and (iii) monomers of 1 and 2 undergo ion–dipole interactions to form a 1:1 molecular complex. If χ_{12} , χ_{22} and χ'_{12} represent molar interaction and molar compressibility interaction parameters for 1–2_n contacts, depolymerization of 2_n components, and ion–dipole interactions between 1 and 2 components, then the change in thermodynamic properties, Y_{12}^E ($Y = H$ or κ_S) is given [48–51] by:

$$Y_{12}^E(Y = \text{Hor } \kappa_S) = \left[\frac{x_1 x_2 \left({}^3\zeta_1 / {}^3\zeta_2 \right)}{x_1 + x_2 \left({}^3\zeta_1 / {}^3\zeta_2 \right)} \right] [\chi_{12}] + \frac{x_1^2 x_2 \left({}^3\zeta_1 / {}^3\zeta_2 \right)}{x_1 + x_2 \left({}^3\zeta_1 / {}^3\zeta_2 \right)} [\chi_{22}] + \left[\frac{x_1 x_2^2 \left({}^3\zeta_1 / {}^3\zeta_2 \right)}{x_1 + x_2 \left({}^3\zeta_1 / {}^3\zeta_2 \right)} \right] [\chi'_{12}] \quad (8)$$

Further, if it is assumed that the interaction parameters for unlike contacts and ion-dipole interactions between the (1) and (2) components are nearly equal, $\chi_{12} \cong \chi_{22} = \chi^*$, then Eq. 8 reduces to:

$$Y_{12}^E (Y = H \text{ or } \kappa_S) = \left[\frac{x_1 x_2 (\xi_1 / \xi_2)^{1/3}}{x_1 + x_2 (\xi_1 / \xi_2)^{1/3}} \right] \left[(1 + x_1) \chi^* + x_2 \chi'_{12} \right] \tag{9}$$

Equation 9 contains two unknown χ^* and χ'_{12} parameters. These parameters were evaluated by using H_{12}^E and $(\kappa_S^E)_{12}$ data at $x_1 = 0.4$ and 0.6 , and were then subsequently utilized to predict H_{12}^E and $(\kappa_S^E)_{12}$ values of (1 + 2) mixtures at other values of x_1 . Such $(\kappa_S^E)_{12}$ and H_{12}^E values of the investigated mixtures are plotted in Figs. 5, 6, 7, 8 and 9, respectively, and are compared with their experimental values. The χ^* and χ'_{12} parameters, along with deviations between experimental V_{12}^E , $(\kappa_S^E)_{12}$ and H_{12}^E values and the corresponding values obtained from Graph theory, are recorded in Table 5. Examination of Figs. 5, 6, 7, 8, 9 reveals that the H_{12}^E and $(\kappa_S^E)_{12}$ values compare well with their experimental values which, in turn, supports the various assumptions made in deriving Eq. 9.

6 Prigogine–Flory–Patterson (PFP) Theory

6.1 Excess Molar Volumes

The PFP theory [52] assumes that V_{12}^E is the sum of three contributions: (i) an interaction contribution, (ii) a free volume contribution, and (iii) an internal pressure contribution.

Each contributing term is given by:

$$\frac{V_{\text{interaction}}^E}{\sum_{i=1}^2 x_i v_i^*} = \frac{[(\tilde{v}^{1/3} - 1) \tilde{v} \psi_1 \theta_2 \chi'_{12}]}{[(4/3) \tilde{v}^{-1/3} - 1] \tilde{v}} \tag{10}$$

$$\frac{V_{\text{free-volume}}^E}{\sum_{i=1}^2 x_i v_i^*} = \left[(\tilde{v}_1 - \tilde{v}_2)^2 \left\{ (14/9) \tilde{v}^{-1/3} - 1 \right\} \right] \frac{\psi_1 \psi_2}{[(4/3) \tilde{v}^{-1/3} - 1] \tilde{v}} \tag{11}$$

$$\frac{V_{P^* \text{effect}}^E}{\sum_{i=1}^2 x_i v_i^*} = \frac{(\tilde{v}_1 - \tilde{v}_2) (P_1^* - P_2^*) \psi_1 \psi_2}{(P_1^* \psi_2 - P_2^* \psi_1)} \tag{12}$$

6.2 Excess Molar Enthalpies

According to the PFP theory [53], H_{12}^E values are due to interaction contributions as well as free volume contributions and are expressed by:

$$H_{12}^E = H_{\text{interaction}}^E + H_{\text{free-volume}}^E \tag{13}$$

where

$$\frac{H_{\text{interaction}}^E}{(x_1 U_1^* + x_2 U_2^*)} = \left(\frac{\chi_{12} \theta_2 \psi_1}{P_1^*} \right) (\tilde{U} \tilde{T}_U + \tilde{T}_U \tilde{C}_P \tilde{T}_U) \quad (14)$$

$$\frac{H_{\text{free-volume}}^E}{(x_1 U_1^* + x_2 U_2^*)} = \tilde{C}_p(\tilde{T}_U) (\psi_1 \tilde{T}_1 + \psi_2 \tilde{T}_2 - \tilde{T}_U) \quad (15)$$

6.3 Excess Isentropic Compressibilities

The quantity $(\kappa_S)_{12}$ is given [54] by:

$$(\kappa_S)_{12} = -\frac{1}{V} \left(\frac{\partial V}{\partial p} \right)_S \quad (16)$$

where

$$\left(\frac{\partial V}{\partial p} \right)_S = \left(\frac{\partial V}{\partial p} \right)_T + T C_p^{-1} \left(\frac{\partial V}{\partial T} \right)_p \quad (17)$$

$\left(\frac{\partial V}{\partial p} \right)_T$ and $\left(\frac{\partial V}{\partial T} \right)_p$ are expressed by Eqs. 18 and 19, respectively, where

$$\left(\frac{\partial V}{\partial p} \right)_T = \left(\frac{-\tilde{v}^{7/3} + 2\tilde{v}^2 - \tilde{v}^{5/3}}{4/3 - \tilde{v}^{1/3}} \right) \frac{V^*}{p^* \tilde{T}} \quad (18)$$

$$\left(\frac{\partial V}{\partial T} \right)_p = \left(\frac{\tilde{v}^{4/3} - \tilde{v}}{4/3 - \tilde{v}^{1/3}} \right) \frac{V^*}{T} \quad (19)$$

All of the terms in Eqs. 10–19 have the same significance as described elsewhere [55, 56].

The V_{12}^E , H_{12}^E and $(\kappa_S^E)_{12}$ values by PFP theory can be predicted if the interaction energy parameter χ_{12}^* , in addition to the Flory's parameters and isobaric heat capacities of the pure liquids and mixtures, are known. The interaction parameter χ_{12}^* was determined by fitting of the H_{12}^E value of investigated (1 + 2) mixtures at $x_1 = 0.5$ to Eq. 21:

$$H_{12}^E = \sum x_i p_i^* (U_i^{-1} - U_{\text{cal}}^{-1}) + x_1 U_1^* \theta_2 \chi_{12}^* U_{\text{cal}}^{-1} \quad (20)$$

The various parameters for the pure components were determined using isothermal compressibility results reported in the literature [22, 29, 33–35]. The κ_T values for [emim][BF₄] were predicted in the manner described elsewhere [40, 57], and for NMF and DMF were determined by using their ΔH_v values [58]. Such V_{12}^E , $(\kappa_S^E)_{12}$ and H_{12}^E values are plotted in Figs. 1, 2, 3, 4, 5, 6, 7, 8 and 9, respectively. Further, the interaction energy parameter χ_{12}^* , along with deviations between experimental V_{12}^E , $(\kappa_S^E)_{12}$ and H_{12}^E values and the corresponding values obtained from PFP theory are reported in Table 6. Examination of Figs. 1, 2, 3, 4, 5, 6, 7, 8, 9 reveals that the PFP theory correctly predicts the sign of V_{12}^E , H_{12}^E and $(\kappa_S^E)_{12}$ values for all of the studied mixtures. However, quantitative agreement is not as impressive as compared to the values predicted by Graph theory. The failure of the PFP theory to correctly predict the magnitude of V_{12}^E , H_{12}^E and $(\kappa_S^E)_{12}$ data may be due to strong interactions between unlike molecules in the mixtures. Further, examination of χ_{12}^* values for [emim][BF₄] (1) + NMF or DMF (2) mixtures indicates that, while the χ_{12}^* values for [emim][BF₄] (1) + NMF (2) are positive, those for [emim][BF₄] (1) + DMF (2)

Table 6 Values of the interaction energy, χ_{ij}^* , parameter of the PFP theory along with the standard deviations $\sigma(V^E, \text{PFP})$, $\sigma(\kappa_S^E, \text{PFP})$, and $\sigma(H^E, \text{PFP})$ from experimental values, V_{12}^E , H_{12}^E and $(\kappa_S^E)_{12}$, and the values obtained from the PFP theory

Mixture	T/K	Interaction energy parameter $\chi_{ij}^*/\text{J}\cdot\text{cm}^{-3}$	Standard deviations		
			$\sigma(V^E, \text{PFP})/\text{cm}^3\cdot\text{mol}^{-1}$	$\sigma(\kappa_S^E, \text{PFP})/\text{TPa}^{-1}$	$\sigma(H^E, \text{PFP})/\text{J}\cdot\text{mol}^{-1}$
1-Ethyl-3-methyl imidazolium tetrafluoroborate (1) + <i>N</i> -methylform amide (2)	293.15	22.0	0.2292	25.5	–
	298.15	22.1	0.2157	26.1	61
	303.15	22.3	0.2477	26.2	–
	308.15	22.9	0.3306	26.1	–
1-Ethyl-3-methyl imidazolium tetrafluoroborate(1) + <i>N,N</i> -dimethylform amide (2)	293.15	–31.2	1.1570	29.8	–
	298.15	–31.6	1.1222	31.7	170
	303.15	–31.7	1.2289	45.8	–
	308.15	–32.4	1.4196	34.7	–

are negative. This is probably due to strong self-association of NMF in comparison to DMF, which prevents strong interaction between NMF and [emim][BF₄] leading to the positive value for χ_{12}^* .

7 Conclusion

The experimental density and speed of sound data of the investigated ionic liquid binary mixtures have been utilized to determine V_{12}^E and $(\kappa_S^E)_{12}$. The V_{12}^E , H_{12}^E and $(\kappa_S^E)_{12}$ data have been fitted to Redlich–Kister equation to predict binary adjustable parameters and standard deviations. The V_{12}^E , H_{12}^E and $(\kappa_S^E)_{12}$ data for the studied ionic liquid mixtures have been analyzed in terms of Graph theory. It has been observed that Graph theory, which has been applied for the first time to ionic liquid mixtures, described well the observed thermodynamic properties as well as the state of components in their pure and mixed states. The V_{12}^E , H_{12}^E and $(\kappa_S^E)_{12}$ data have also been analyzed in terms of PFP theory. The agreement between experimental values and the values determined by PFP theory is not impressive, although the sign of the predicted values are the same as the experimental values.

Acknowledgments Soniya is grateful to University Grants Commission (UGC), New Delhi, for the award of Project Fellow. The authors are also grateful to the Head of Chemistry Department and authorities of M. D. University, Rohtak, for providing research facilities.

References

- Li, Q., Zhang, J., Lei, Z., Zhu, J., Zhu, J., Huang, X.: Selection of ionic liquids as entrainers for the separation of ethyl acetate and ethanol. *Ind. Eng. Chem. Res.* **48**, 9006–9012 (2009)
- Sun, X., Dai, S.: Electrochemical investigations of ionic liquids with vinylene carbonate for applications in rechargeable lithium ion batteries. *Electrochim. Acta* **55**, 4618–4626 (2010)
- Lee, J.S., Mayes, R.T., Luo, H.M., Dai, S.: Ionothermal carbonization of sugars in a protic ionic liquid under ambient conditions. *Carbon* **48**, 3364–3368 (2010)

4. Mahurin, S.M., Lee, J.S., Baker, G.A., Luo, H.M., Dai, S.: Performance of nitrile-containing anions in task-specific ionic liquids for improved CO₂/N₂ separation. *J. Membr. Sci.* **353**, 177–183 (2010)
5. Tekin, A., Safarov, J., Shahverdiyev, A., Hassel, E.: (p , ρ , T) Properties of 1-butyl-3-methylimidazolium tetrafluoroborate and 1-butyl-3-methylimidazolium hexafluorophosphate at $T = (298.15 \text{ to } 398.15) \text{ K}$ and pressures up to $p = 40 \text{ MPa}$. *J. Mol. Liq.* **136**, 170–182 (2007)
6. Singh, T., Kumar, A.: Temperature dependence of physical properties of imidazolium based ionic liquids: Internal pressure and molar refraction. *J. Solution Chem.* **38**, 1043–1053 (2009)
7. Trivedi, T.J., Bharmoria, P., Singh, T., Kumar, A.: Temperature dependence of physical properties of amino acid ionic liquid surfactants. *J. Chem. Eng. Data* **57**, 317–324 (2012)
8. Andreatta, A.E., Arce, A., Rodil, E., Soto, A.: Physico-chemical properties of binary and ternary mixtures of ethyl acetate + ethanol + 1-butyl-3-imidazolium bis(trifluoromethylsulfonyl)imide at 298.15 K and atmospheric pressure. *J. Solution Chem.* **39**, 371–383 (2010)
9. Domańska, U., Laskowska, M.: Effect of temperature and composition on the density and viscosity of binary mixtures of ionic liquids with alcohols. *J. Solution Chem.* **38**, 779–799 (2009)
10. Anouti, M., Vigeant, A., Jacquemin, J., Brigouleix, C., Lemordant, D.: Volumetric properties, viscosity and refractive index of the protic ionic liquids, pyrrolidinium octanoate in molecular solvents. *J. Chem. Thermodyn.* **42**, 834–845 (2010)
11. Hosoya, H.: Topological nature of structure isomers of saturated hydrocarbons. *Bull. Chem. Soc. Jpn.* **44**, 2332–2339 (1971)
12. Balaban, A.T.: Highly discriminating distance-based topological index. *Chem. Phys. Lett.* **89**, 399–404 (1982)
13. Schultz, H.P.: Topological organic chemistry. 1. Graph theory and topological indices of alkanes. *J. Chem. Inf. Comput. Sci.* **29**, 227–228 (1989)
14. Wiener, H.: Structure determination of paraffin boiling points. *J. Am. Chem. Soc.* **69**, 17–20 (1947)
15. Kier, L.B., Hall, L.H.: Molecular Structure Description. The Electrotological State. Academic Press, New York (1999)
16. Saini, N., Jangra, S.K., Yadav, J.S., Sharma, D., Sharma, V.K.: Thermodynamic properties of binary mixtures of tetrahydropyran with pyridine and isomeric picolines: Excess molar volumes, excess molar enthalpies and excess isentropic compressibilities. *Thermochim. Acta* **518**, 13–26 (2011)
17. Sharma, D., Yadav, J.S., Singh, K.C., Sharma, V.K.: Molar excess volumes and excess isentropic compressibilities of ternary mixtures containing *o*-toluidine. *J. Solution Chem.* **37**, 1099–1112 (2008)
18. Sharma, V.K., Siwach, R.K.: Dimple: excess molar volumes, excess molar enthalpies and excess isentropic compressibilities of tetrahydropyran with aromatic hydrocarbons. *J. Chem. Thermodyn.* **43**, 39–46 (2011)
19. Jangra, S.K., Yadav, J.S., Neeti, Dimple, Sharma, V.K.: Thermodynamic properties of liquid mixtures containing 1,3-dioxolane and anilines: Excess molar volumes, excess molar enthalpies, excess Gibbs free energy and isentropic compressibilities changes of mixing. *Thermochim. Acta* **511**, 74–81 (2010)
20. Neeti, Jangra, S.K., Sharma, D., Sharma, V.K.: Excess molar enthalpies of ternary mixtures containing *o*-toluidine + tetrahydropyran with pyridine or isomeric picolines or benzene or toluene at 308.15 K. *Thermochim. Acta* **531**, 28–34 (2012)
21. Scholz, E.: Karl Fischer Titration. Springer, Berlin (1984)
22. Riddick, J.A., Bunger, W.B., Sankano, T.K.: Techniques in Chemistry, 4th edn. Wiley, New York (1986)
23. Vogel, A.I.: A Text Book of Practical Organic Chemistry, 5th edn, p. 409. English Book Society and Longman Group, London (2003)
24. Curras, M.R., Gomes, M.F.C., Husson, P., Padua, A.A.H., Garcia, J.: Calorimetric and volumetric study on binary mixtures 2,2,2-trifluoroethanol + (1-butyl-3-methylimidazolium tetrafluoroborate or 1-ethyl-3-methylimidazolium tetrafluoroborate). *J. Chem. Eng. Data* **55**, 5504–5512 (2010)
25. Navia, P., Troncoso, J., Romani, L.: Excess magnitudes for ionic liquid binary mixtures with a common ion. *J. Chem. Eng. Data* **52**, 1369–1374 (2007)
26. Stoppa, A., Zech, O., Kunz, W., Buchner, R.: The conductivity of imidazolium-based ionic liquids from (–35 to 195) °C. A variation of cation's alkyl chain. *J. Chem. Eng. Data* **55**, 1768–1773 (2010)
27. Nikolic, A., Jovic, B., Krstic, V., Trickovic, J.: Excess molar volume of N-methylformamide + tetrahydropyran + 2-pentanone + *n*-propylacetate at the temperature between 298.15 and 313.15 K. *J. Mol. Liq.* **133**, 39–42 (2007)
28. Papamatthaiakis, D., Aroni, F., Havredaki, V.: Isentropic compressibilities of (amide + water) mixtures: a comparative study. *J. Chem. Thermodyn.* **40**, 107–118 (2008)
29. Checoni, R.F.P., Volpe, L.O.: Measurements of the molar heat capacities and excess molar heat capacities for water + organic solvents mixtures at 288.15 to 303.15 K and atmospheric pressure. *J. Solution Chem.* **39**, 259–279 (2010)

30. Chu, D.Y., Chang, Y., Hu, I.Y., Liu, R.L.: Excess molar volumes of mixtures of *N, N*-dimethylformamide and water and apparent molal volumes and partial molal volumes of *N, N*-dimethylformamide in water from 278.15 K to 318.15 K. *Wuli Huaxue Xuebao* **6**, 203–208 (1990)
31. Marchetti, A., Preti, C., Tagliazucchi, M., Tassi, L., Tosi, G.J.: The *N, N*-dimethylformamide/ethane-1,2-diol solvent system, density, viscosity, and excess molar volume at various temperatures. *Chem. Eng. Data* **36**, 360–365 (1991)
32. Murthy, N.M., Siva Kumar, K.V., Rajagopal, E., Subrahmanyam, S.V.: Excess thermodynamic and water–*N, N*-dimethylformamide. *Acustica* **48**, 341–345 (1981)
33. Neeti, Yadav, J.S., Jangra, S.K., Dimple, Sharma, V.K.: Thermodynamic studies of molecular interactions in mixtures of *o*-toluidine with pyridine and picolines: excess molar volumes, excess molar enthalpies and excess isentropic compressibilities. *J. Chem. Thermodyn.* **43**, 782–795 (2011)
34. Dubey, G.P., Sharma, M.: Temperature and composition dependence of the densities, viscosities, and speeds of sound of binary liquid mixtures of 1-butanol with hexadecane and squalane. *J. Chem. Eng. Data* **53**, 1032–1038 (2008)
35. Dimple, Yadav, J.S., Singh, K.C., Sharma, V.K.: Molecular interaction in binary mixture containing *o*-toluidine. *Thermochim. Acta* **468**, 108–115 (2008)
36. Benson, G.C., Kiyohara, O.: Evaluation of excess isentropic compressibilities and isochoric heat capacities. *J. Chem. Thermodyn.* **11**, 1061–1064 (1979)
37. Sanmamed, Y.A., Navia, P., Salgado, D.G., Troncoso, J., Romani, L.: Pressure and temperature dependence of isobaric heat capacity for [Emim][BF₄], [Bmim][BF₄], [Hmim][BF₄] and [Omim][BF₄]. *J. Chem. Eng. Data* **55**, 600–604 (2010)
38. Lide, D.: *Handbook of Chemistry and Physics*, 83rd edn. CRC Press, Boca Raton (2002)
39. Reid, T.M., Praunitz, J.M., Poling, B.E. (eds.): *The Properties of Gases and Liquids*, 4th edn. McGraw Hill, New York (1987)
40. Brocos, P., Amigo, A., Points, M., Calvo, E., Bravo, R.: Application of the Prigogine–Flory–Patterson model to excess volumes of mixtures of tetrahydrofuran or tetrahydropyran with cyclohexane or toluene. *Thermochim. Acta* **286**, 297–306 (1996)
41. Singh, P.P., Sharma, V.K., Sharma, S.P.: Topological studies of the molecular species that characterize lower alkanols + methylene bromide mixtures: molar excess volumes and molar excess enthalpies. *Thermochim. Acta* **106**, 293–307 (1986)
42. Singh, P.P.: Topological aspects of the effect of temperature and pressure on the thermodynamics of binary mixtures of non-electrolytes. *Thermochim. Acta* **66**, 37–73 (1983)
43. Kier, L.B., Yalkowsky, S.H., Sinkula, A.A., Valvani, S.C.: *Physico-chemical Properties of Drugs*, Chap. 9, p. 282. Merceel Dekker, New York (1980)
44. Katsyuba, S.A., Dyson, P.J., Vandyukova, E.E., Chernova, A.V., Vidis, A.: Molecular structure, vibrational spectra, and hydrogen bonding of the ionic liquid 1-ethyl-3-methyl-1*H*-imidazolium tetrafluoroborate. *Helv. Chim. Acta* **87**, 2556–2565 (2004)
45. Meng, Z., Dolle, A., Carper, W.R.: Gas phase model of the ionic liquid: semi-empirical and ab initio bonding and molecular structure. *J. Mol. Struct. (Theochem)* **585**, 119–128 (2002)
46. Morrow, T.I., Maginn, E.J.: Molecular dynamics study of the ionic liquid 1-*n*-butyl-3-methylimidazolium hexafluorophosphate. *J. Phys. Chem B* **106**, 12807–12813 (2002)
47. Rao, C.N.R.: *Chemical Application of Infrared Spectroscopy*. Academic Press, London (1963)
48. Huggins, M.L.: The thermodynamic properties of liquids included solutions: part 1. Intermolecular energies in mono atomic liquids and their mixtures. *J. Phys. Chem.* **74**, 371–378 (1970)
49. Huggins, M.L.: The thermodynamic properties of liquids included solutions: part 2. Polymer solutions considered as diatomic system. *Polymer* **12**, 389–399 (1971)
50. Singh, P.P., Bhatia, M.: Energetic of molecular interactions in binary mixtures of non-electrolytes containing a salt. *J. Chem. Soc. Faraday Trans I* **85**, 3807–3812 (1989)
51. Singh, P.P., Nigam, R.K., Singh, K.C., Sharma, V.K.: Topological aspects of the thermodynamics of binary mixtures of non-electrolytes. *Thermochim. Acta* **46**, 175–190 (1981)
52. Van, H.T., Patterson, D.: Volume of mixing and P^* effect: part 1. Hexane isomers with normal and branched hexadecane. *J. Solution Chem.* **11**, 793–805 (1982)
53. Galvao, A.C., Francesconi, A.Z.: Applications of the Prigogine–Flory–Patterson model to excess molar enthalpy of binary liquid mixtures containing acetonitrile and alkanols. *J. Mol. Liq.* **139**, 110–116 (2008)
54. Oswal, S.L., Maisuria, M.M.: Speed of sound isentropic compressibilities and excess molar volumes and aromatic hydrocarbon at 303.15 K. I. Results for cycloalkane + cycloalkanes, and cycloalkane + alkanes. *J. Mol. Liq.* **100**, 91–112 (2002)
55. Flory, P.J.: The statistical thermodynamic of liquid mixtures. *J. Am. Chem. Soc.* **87**, 1833–1838 (1965)

56. Flory, P.J.: The thermodynamic properties of mixture of small non-polar molecules. *J. Am. Chem. Soc.* **87**, 1838–1846 (1965)
57. Kabo, G.J., Blokhin, A.V., Paulechka, Y.U., Kabo, A.G., Shymanovich, M.P., Magee, J.W.: Thermodynamic properties of 1-butyl-3-methylimidazolium hexafluorophosphate in the condensed state. *J. Chem. Eng. Data* **49**, 453–461 (2004)
58. Hildebrand, J.H., Prusnitz, J.M., Scott, R.L.: *Regular and Related Solutions: The Solubility of Gases, Liquids, and Solids*. Van-Nonstand Reinheld, New York (1971)